9584–9595 *Nucleic Acids Research, 2012, Vol. 40, No. 19* *Published online 27 July 2012*
doi:10.1093/nar/gks715

The ATPase activity of Fml1 is essential for its roles in homologous recombination and DNA repair

Saikat Nandi and Matthew C. Whitby*

Department of Biochemistry, University of Oxford, Oxford OX1 3QU, UK

Received February 9, 2012; Revised June 18, 2012; Accepted July 3, 2012

ABSTRACT

In fission yeast, the DNA helicase Fml1, which is an orthologue of human FANCM, is a key component of the machinery that drives and governs homologous recombination (HR). During the repair of DNA double-strand breaks by HR, it limits the occurrence of potentially deleterious crossover recombinants, whereas at stalled replication forks, it promotes HR to aid their recovery. Here, we have mutated conserved residues in Fml1's Walker A (K99R) and Walker B (D196N) motifs to determine whether its activities are dependent on its ability to hydrolyse ATP. Both Fml1^{K99R} and Fml1^{D196N} are proficient for DNA binding but totally deficient in DNA unwinding and ATP hydrolysis. *In vivo* both mutants exhibit a similar reduction in recombination at blocked replication forks as a *fml1*Δ mutant indicating that Fml1's motor activity, fuelled by ATP hydrolysis, is essential for its pro-recombinogenic role. Intriguingly, both *fml1*^{K99R} and *fml1*^{D196N} mutants exhibit greater sensitivity to genotoxins and higher levels of crossing over during DSB repair than a *fml1*Δ strain. These data suggest that without its motor activity, the binding of Fml1 to its DNA substrate can impede alternative mechanisms of repair and crossover avoidance.

INTRODUCTION

The FANCM family of DNA helicases/translocases plays key roles in homologous recombination (HR) and DNA repair in archaea and eukaryotes (1). Human FANCM is a component of a network of DNA repair proteins, which if mutated can result in the genetic disease Fanconi anaemia (FA) characterized by progressive bone marrow failure, various developmental abnormalities and cancer predisposition (2). A distinguishing feature of FA is cellular hypersensitivity to agents that cause DNA interstrand crosslinks (ICLs) such as mitomycin C and cisplatin indicating an underlying defect in the repair of this class of lesion (3–5). A key role for FANCM in ICL repair appears to be to promote the recruitment of the FA core complex (consisting of FANCA, B, C, E, F, G and L) to replication forks that are stalled at ICLs (6,7). The core complex then promotes the monoubiquitination of FANCD2 and FANCI, which is thought to activate them for the co-ordination of downstream repair pathways including HR and translesion DNA synthesis (TLS) (3–5). However, a series of genetic studies have shown that FANCM's role in the repair/tolerance of DNA damage is not restricted to an involvement with the FA core complex. Additional roles include promoting the S-phase checkpoint (8–10), possibly by acting as a sensor of stalled/broken replication forks and/or regulating the loading of RPA, and limiting sister chromatid exchange (11–13), which indicates that it has a role in controlling HR. At least some of these FA core complex-independent roles are conserved in lower eukaryotes. For example, yeast orthologues of FANCM (Mph1 in *Saccharomyces cerevisiae* and Fml1 in *Schizosaccharomyces pombe*) play a prominent role in limiting crossover recombinants during mitotic DNA double-strand break (DSB) repair, and in the case of Fml1, there is good evidence for its involvement in processing stalled replication forks (14,15).

The FANCM family are Superfamily 2 (SF2) helicases/translocases and as such are characterized by seven conserved motifs including a Walker A motif (motif I) that binds the triphosphate tail of ATP and a DEAH box (motif II), which is a version of the Walker B motif that binds magnesium ions and consequently plays an essential role in catalysing ATP hydrolysis (1). *In vitro* studies of purified FANCM family proteins have provided insight into how their various *in vivo* functions might be performed. A general ability to unwind and/or branch migrate DNA junctions that resemble intermediates of HR and stalled replication forks has been noted. In particular, FANCM family members are proficient at branch migrating Holliday junctions (HJs) and unwinding

*To whom correspondence should be addressed. Tel: +44 1865 613239; Fax: +44 1865 613343; Email: matthew.whitby@bioch.ox.ac.uk

displacement (D)-loops that are formed by Rad51-mediated strand invasion (14–18). The latter activity shows how they could be capable of promoting a form of DSB repair called synthesis dependent strand annealing (SDSA), which involves D-loop dissociation and generates solely non-crossover recombinants (1). A failure of SDSA can lead to an increase in crossover recombinants through the cleavage of D-loops and HJs by junction-specific endonucleases (19).

In addition to an ability to unwind D-loops, FANCM family members are also adept at catalysing replication fork reversal (15,16,18,20). This reaction involves the unwinding of both nascent strands at a stalled replication fork followed by their annealing and the re-annealing of the parental strands. This activity may serve several functions including: (i) facilitating DNA repair by providing space for the excision of strand lesions that block fork progression; (ii) providing a means of tolerating DNA damage by enabling the DNA polymerase to switch from the damaged template strand to the undamaged equivalent nascent strand and thereby bypass the lesion and (iii) promoting recombination-dependent replication restart by generating a double-stranded (ds) DNA end, which can act as an entry point for recombinases. Consistent with a role in catalysing fork reversal Fml1 has been shown to promote Rad51-dependent recombination at a blocked replication fork *in vivo* (15,20).

The ability of various FANCM family members to unwind D-loops and reverse replication forks *in vitro* depends on a supply of hydrolysable ATP (1). Mutations that impair ATP hydrolysis in FANCM and Mph1 have been shown to confer deficiencies in DNA repair and crossover avoidance *in vivo* (12,14). However, in some cases, biological activity is not destroyed presumably because FANCM can also act as a molecular scaffold for the recruitment of proteins (7,8,12,21). Here, we determine whether Fml1's roles in DNA repair, crossover avoidance and processing stalled replication forks are dependent on its ability to hydrolyse ATP.

MATERIALS AND METHODS

Schizosaccharomyces pombe strains and plasmids

Schizosaccharomyces pombe strains are listed in Table 1. The *fml1*$^{+}$::*natMX4* strain was made by gene targeting using a derivative of pAG25 (22), which was constructed as follows. First, the *ADH1* terminator from pFA6a-GST-kanMX6 was sub-cloned as a *Asc*I-*Bgl*II fragment into pAG25 to make pMW756. A ~300 bp *Sac*I-*Eco*RI fragment from the *fml1* 3′-UTR region was then sub-cloned from pMW778 into pMW756 to make pSN13. A *Sal*I-*Sma*I fragment encompassing the entire *fml1*$^{+}$ open reading frame (ORF) was then sub-cloned from pMW848 (see below) into the *Sal*I and *Pac*I (blunt-ended by Klenow) sites in pSN13 to make pSN14. The gene-targeting fragment was excised from pSN14 by digestion with *Sal*I and partial digestion with *Xba*I. Derivatives of pSN14, in which either an A296G (pSN16) or G586A (pSN15) point mutation was introduced into *fml1*$^{+}$ using QuikChange XL site-directed mutagenesis (Agilent Technologies, CA), were used to make the *fml1*^{K99R}::*natMX4* and *fml1*^{D196N}::*natMX4* strains. The *fml1*$^{+}$-*GFP*::*natMX4* strain was made by gene targeting using a derivative of pFA6a-GFP(S65T)-kanMX6 (23), which was constructed as follows. First, a *Bgl*II-*Eco*RV fragment containing the *natMX4* and *fml1* 3′-UTR from pSN13 was sub-cloned into pFA6a-GFP(S65T)-kanMX6. The 3′-end of the *fml1* ORF was then amplified from genomic DNA using oMW1004 (5′-AGAAAGGCTGCTGGAATGTC-3′) and oMW 1005 (5′-TATTTAATTAAAATCAGCATTCCTTTCAT ACG-3′) and cloned as a *Nde*I-*Pac*I fragment into this plasmid to make pJBB31. The gene-targeting fragment was excised from pJBB31 by digestion with *Nde*I and *Xba*I. To construct the *fml1*^{K99R}-*GFP*::*natMX4* and *fml1*^{D196N}-*GFP*::*natMX4* strains, *fml1*^{K99R}::*natMX4* and *fml1*^{D196N}::*natMX4* strains were first converted to *fml1*^{K99R}::*hphMX4* and *fml1*^{D196N}::*hphMX4*, respectively, by gene targeting using a *Bam*HI-*Eco*RV fragment from pAG32 containing the hygromycin resistance gene. The resultant strains were then subjected to gene targeting using the *Nde*I and *Xba*I fragment from pJBB31 as described earlier. The plasmid for expressing His-tagged Fml1ΔC in *Escherichia coli* was pSN3 and has been described previously (15). Expression plasmids for His-tagged Fml1ΔC^{K99R} (pSN5) and Fml1ΔC^{D196N} (pSN4) were derived from pSN3 by site-directed mutagenesis as described earlier. pREP41-Fml1ΔC (pMW856) has been described (15). pREP41-Fml1ΔC^{K99R} (pSN22) and pREP41ΔC^{D196N} (pSN21) were derived from pMW856 by site-directed mutagenesis as described earlier. pREP41-Fml1 (pMW848) was constructed by amplifying full-length *fml1* from genomic DNA, using primers oMW873 (5′-TATTAGTCGACATGTCCGATGATTCT TTTAG-3′) and oMW874 (5′-TATTCCCGGGATTCTC TAAATCAGCATTCC-3′) and cloning it as a *Sal*I-*Sma*I fragment into pREP41 (24). pREP41-Fml1^{K99R} (pSN23) and pREP41^{D196N} (pSN24) were derived from pMW848 by site-directed mutagenesis as described earlier. All plasmids were verified by DNA sequencing.

Media and genetic methods

Media and genetic methods followed standard protocols (25). The complete and minimal media were yeast extract with supplements (YES) and Edinburgh minimal medium plus 3.7 mg/ml sodium glutamate (EMMG) plus appropriate amino acids (0.25 mg/ml), respectively. Low adenine media (YELA) was supplemented with 0.01 mg/ml adenine. Ade^{+} recombinants were selected on YES lacking adenine and supplemented with 0.2 mg/ml guanine to prevent uptake of residual adenine.

Spot assays

Exponentially growing cells from liquid cultures were harvested, washed and re-suspended in water at a density of 1×10^{7}–1×10^{3} cells/ml. Aliquots (10 µl) of the cell suspensions were spotted onto agar plates containing genotoxins as indicated. For UV, plates were irradiated using a Stratalinker (Stratagene). Plates were photographed after 4 days growth at 30°C unless otherwise indicated.

Table 1. *Schizosaccharomyces pombe* strains used in this study

Strain	Relevant genotype	Source
MCW1221	*h⁺ ura4-D18 leu1-32 his3-D1 arg3-D4*	Laboratory strain
MCW2080	*h⁺ fml1Δ::natMX4 ura4-D18 leu1-32 his3-D1 arg3-D4*	(15)
MCW4581	*h⁺ fml1⁺::natMX4 ura4-D18 leu1-32 his3-D1 arg3-D4*	This study
MCW4778	*h⁺ fml1^{D196N}::natMX4 ura4-D18 leu1-32 his3-D1 arg3-D4*	This study
MCW4779	*h⁺ fml1^{K99R}::natMX4 ura4-D18 leu1-32 his3-D1 arg3-D4*	This study
MCW1193	*h⁺ ura4-D18 leu1-32 his3-D1 arg3-D4 ade6-M26*	Laboratory strain
MCW2096	*h⁺ fml1Δ::natMX4 ura4-D18 leu1-32 his3-D1 arg3-D4 ade6-M26*	(15)
MCW4893	*h⁺ fml1⁺::natMX4 ura4-D18 leu1-32 his3-D1 arg3-D4 ade6-M26*	This study
MCW4894	*h⁺ fml1^{D196N}::natMX4 ura4-D18 leu1-32 his3-D1 arg3-D4 ade6-M26*	This study
MCW4895	*h⁺ fml1^{K99R}::natMX4 ura4-D18 leu1-32 his3-D1 arg3-D4 ade6-M26*	This study
MCW4713	*h⁺ ura4-D18 leu1-32 his3-D1 arg3-D4 ade6-M375 int::pUC8/his3⁺/RTS1 site A orientation 2/ade6-L469*	Laboratory strain
MCW3061	*h⁺ fml1Δ::natMX4 ura4-D18 leu1-32 his3-D1 arg3-D4 ade6-M375 int::pUC8/his3⁺/RTS1 site A orientation 2/ade6-L469*	(15)
MCW4797	*h⁺ fml1⁺::natMX4 ura4-D18 leu1-32 his3-D1 arg3-D4 ade6-M375 int::pUC8/his3⁺/RTS1 site A orientation 2/ade6-L469*	This study
MCW4780	*h⁺ fml1^{K99R}::natMX4 ura4-D18 leu1-32 his3-D1 arg3-D4 ade6-M375 int::pUC8/his3⁺/RTS1 site A orientation 2/ade6-L469*	This study
MCW4801	*h⁺ fml1^{D196N}::natMX4 ura4-D18 leu1-32 his3-D1 arg3-D4 ade6-M375 int::pUC8/his3⁺/RTS1 site A orientation 2/ade6-L469*	This study
MCW4836	*h⁺ fml1⁺-GFP::natMX4 ura4-D18 leu1-32 his3-D1 arg3-D4*	This study
MCW6137	*h⁺ fml1^{D196N}-GFP::natMX4 ura4-D18 leu1-32 his3-D1 arg3-D4*	This study
MCW6138	*h⁺ fml1^{K99R}-GFP::natMX4 ura4-D18 leu1-32 his3-D1 arg3-D4*	This study

Microscopy

Cells from an overnight culture in YES were harvested, washed in water, re-suspended in fresh YES and grown for 3 h at 30°C before addition of 0.03% methyl methane sulphonate (MMS). Incubation was continued for a further 4 h before the cells were harvested and washed to remove the MMS. They were then re-suspended in fresh YES and allowed to recover at 30°C. Samples were taken at hourly intervals and fixed with 70% ethanol for subsequent microscopy. The fixed cells were stained with DAPI and analysed using an Olympus BX50 epifluorescence microscope equipped with the appropriate filter sets to detect blue and green fluorescence (Chroma Technology Corp., VT). Black and white images were acquired with a CoolSNAP HQ CCD camera (Photometrics, AZ) controlled by MetaMorph software (v7.7.3.0, Molecular Devices Inc., CA).

Recombination assays

The direct repeat recombination assay and plasmid gap repair assay were performed as described (15,26,27). Two sample *t*-tests were used to determine the statistical significance of differences in recombination values between strains.

Protein purification

Wild-type and mutant Fml1ΔC were purified as described (15). Amounts of protein are expressed in moles of monomer, and were estimated using a Bio-Rad protein assay kit with bovine serum albumin (BSA) as the standard.

ATPase assay

Reaction mixtures (20 µl) contained 5 nM wild-type or mutant Fml1ΔC protein, 2.5 mM $MgCl_2$ and 200 nM PhiX174 circular single-stranded (ss) DNA (New England Biolabs) in buffer (25 mM Tris–HCl, pH 8.0, 1 mM dithiothreitol (DTT), 100 µg/ml BSA, 6% glycerol). Reactions were started by the addition of 5 mM ATP and then incubated at 37°C for 30 min before being stopped by the addition of 5 µl of 200 mM ethylenediaminetetraacetic acid (EDTA). The extent of ATP hydrolysis was determined by measuring the amount of inorganic phosphate that had been released into the reaction mixture using a malachite green colourimetric assay based on that developed by Baykov *et al*. (28). In brief malachite green solution (0.5 mM malachite green oxalate, 0.1 N HCl) was mixed with ammonium molybdate solution (34 mM ammonium molybdate tetrahydrate, 4 N HCl) in a 3:1 ratio and filtered through two 0.22 µM filters to make the colourmetric reagent, which was stored in the dark; 700 µl of the colourmetric reagent was added to the stopped reaction mixture and incubated for 1 min at room temperature. The development of colour was then stopped by addition of 200 µl 34% (w/v) sodium citrate followed by mixing using a vortex mixer. Absorbance of the mixture at 610 nm was then measured and the amount of inorganic phosphate determined by reference to known standards.

DNA substrates

The ^{32}P-labelled DNA substrates in Figure 2, Supplementary Figures S1 and S3 were made by annealing the following combination of oligonucleotides: X-12, oligonucleotides 1–4; linear dsDNA, oligonucleotides 2 and oMW96; X0, oligonucleotides 2, 5, 6 and 7; fork, oligonucleotides 2, 5 and 11. Oligonucleotides 1–7 and 11, and the method of substrate preparation have been described (29,30). The sequence of oligonucleotide oMW96 is 5′-CA ACGTCATAGACGATTACATTGCTAGGACATCTT TGCCCACGTTGACCC-3′. Oligonucleotides were supplied by Sigma-Genosys Ltd. and were purified as described (31). The model replication fork in Figure 3

was constructed from two nearly identical plasmids pG46 and pG68 as described (32,33). In brief, differently sized complementary single-strand gaps were introduced into each plasmid using the nicking endonucleases Nt.BbvCI and Nb.BbvCI. One of the plasmids (pG46) was then radiolabelled with ^{32}P at its free 5′ and the other (pG68) linearized by *Xho*I digestion. The two plasmids were then annealed and model replication forks separated from non-annealed DNA by agarose gel electrophoresis followed by purification using a QIAquick Gel Extraction Kit (Qiagen).

DNA-binding assays

Reaction mixtures (20 µl) contained 0.5 nM labelled X-12 in buffer (25 mM Tris–HCl, pH 8.0, 1 mM DTT, 100 µg/ml BSA, 6% glycerol) plus wild-type or mutant Fml1ΔC protein as indicated. Reactions were incubated on ice for 15 min and then loaded onto a 4% native polyacrylamide gel in low ionic strength buffer (6.7 mM Tris–HCl, pH 8.0, 3.3 mM sodium acetate, 2 mM EDTA) that had been pre-cooled at 4°C. Gels were run for 1 h and 45 min at 160 V with continuous buffer recirculation. Gels were then dried on 3 mm Whatman paper and analysed by Phosphor Imaging using a Fuji FLA3000 and Image Gauge software.

DNA unwinding assay

Reaction mixtures (20 µl) contained 0.5 nM labelled substrate DNA in buffer (50 mM Tris–HCl, pH 8.0, 1 mM DTT, 100 µg/ml BSA, 6% glycerol) plus 2.5 mM $MgCl_2$, 5 mM ATP and protein as indicated. Reactions were incubated at 30°C for 30 min and then terminated by adding one-fifth volume of stop mix (2.5% sodium dodecyl sulphate, 200 mM EDTA, 10 mg/ml proteinase K) and incubating for a further 15 min at 37°C to deproteinize the mixture. Reaction products were separated by electrophoresis through a 10% native polyacrylamide gel at 200 V in TBE buffer. The gel was dried on 3 mm Whatman paper and analysed by Phosphor Imaging using a Fuji FLA3000 and Image Gauge software.

Fork regression assay

Reaction mixtures (40 µl) contained 5 nM of the plasmid-sized labelled fork substrate in buffer (50 mM Tris–HCl, pH 8.0, 1 mM DTT, 100 µg/ml BSA, 6% glycerol) plus 2.5 mM $MgCl_2$, 5 mM ATP and 5 nM of wild-type or mutant Fml1ΔC. Reactions were incubated for 30 min at 30°C after which samples were taken and digested with the indicated restriction enzymes (note that the excess magnesium ions in the restriction enzyme buffers effectively stops the fork regression reaction). The digested samples were separated by electrophoresis through a 10% native polyacrylamide gel. The gel was dried on 3 mm Whatman paper and analysed by Phosphor Imaging using a Fuji FLA3000 and Image Gauge software.

RESULTS

DNA-binding and ATPase activities of Fml1

Full-length Fml1 is insoluble when produced in *E. coli*, and therefore to study its biochemical activities *in vitro,* we purified a C-terminally truncated form of it (Fml1ΔC), which contains the entire helicase domain (Figure 1A and B). Fml1ΔC is able to fully complement the hypersensitivity of a *fml1*Δ mutant to the alkylating agent MMS when over-expressed, demonstrating that it retains its core biological activity (15).

Fml1ΔC binds well to a range of different branched DNA structures *in vitro*, including model replication forks, D-loops and HJs (15). It also binds well to ssDNA but poorly to linear dsDNA (Supplementary Figure S1A). This suggests that Fml1ΔC's ability to bind branched DNA could simply be a consequence of its ssDNA-binding activity. However, Fml1ΔC binds well to the static HJ X0, which is composed of duplex DNA that is not prone to extensive base-pair 'breathing' (34), indicating a genuine specificity for branched DNA molecules over linear duplex DNA (Supplementary Figure S1A). Indeed, its binding to ssDNA could be due to interaction with DNA secondary structures rather than to ssDNA itself. Consistent with its DNA-binding preference, Fml1ΔC exhibits a DNA-dependent ATPase activity that is stimulated more strongly by ssDNA than by dsDNA (Supplementary Figure S1B).

ATPase-deficient mutants of Fml1

To investigate the importance of Fml1's ATPase activity, we changed conserved residues in motif I (K99R) and II (D196N) of its helicase domain (Figure 1A and Supplementary Figure S2). C-terminally truncated forms of each mutant protein were purified by the same protocol used previously for wild-type protein (Figure 1A and B) (15). The purified mutant proteins were then compared to wild-type for their ability to hydrolyse ATP in the presence of ssDNA (Figure 1C). During the 30-min reaction, wild-type Fml1ΔC hydrolysed ~2900 pmol of ATP. In contrast, both mutant proteins hydrolysed only 80–90 pmol, which was only just above background levels. The same inability to hydrolyse ATP was also observed when dsDNA was used instead of ssDNA (data not shown). These data show that K99R and D196N mutations in Fml1ΔC disable its DNA-dependent ATPase activity.

Fml1ΔC^{K99R} and Fml1ΔC^{D196N} exhibit normal junction DNA binding but are deficient in dissociating synthetic HJs

To establish the *in vitro* capabilities of the Fml1ΔC^{K99R} and Fml1ΔC^{D196N} proteins they were tested for their ability to bind and dissociate a synthetic HJ (X-12). X-12 is made by annealing four ~50-mer oligonucleotides and contains a 12-bp homologous core, in which the junction point is free to migrate and 18–20 bp heterologous arms that prevent the junction from spontaneously dissociating. To assess binding to X-12, an eletrophoretic mobility shift assay (EMSA) was used. Both wild-type and mutant Fml1ΔC proteins bind to X-12 equally well

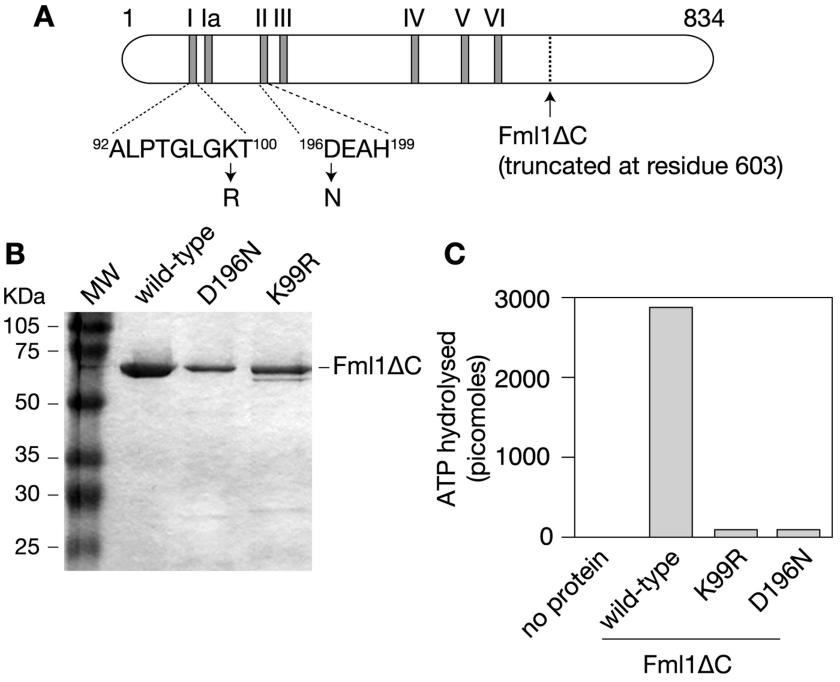

Figure 1. Purification and ATPase activity of wild-type and mutant Fml1ΔCs. (**A**) Schematic of Fml1 showing the position of its helicase motifs, point of truncation in Fml1ΔC and residues mutated to disrupt its ATPase activity. (**B**) Coomassie blue-stained SDS polyacrylamide gel showing purified wild-type and mutant His-tagged Fml1ΔC proteins. (**C**) Comparison of the amount ATP hydrolysed by wild-type and mutant Fml1ΔC proteins. See 'Materials and Methods' section for further details.

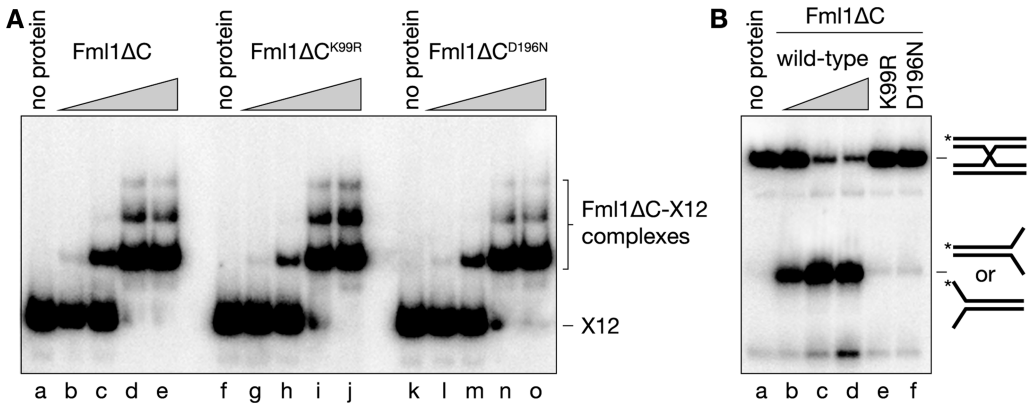

Figure 2. Binding and unwinding X-12 by wild-type and mutant Fml1ΔCs. (**A**) Electrophoretic mobility shift assay showing the binding of X-12 by increasing amounts of Fml1ΔC (lanes b–e: 0.05, 0.5, 5 and 10 nM), Fml1ΔC^{K99R} (lanes g–j: 0.05, 0.5, 5 and 10 nM) and Fml1ΔC^{D196N} (lanes l–o: 0.05, 0.5, 5 and 10 nM). See 'Materials and Methods' section for further details. (**B**) Comparison of X-12 unwinding by Fml1ΔC (lanes b–d: 0.05, 0.5 and 5 nM) Fml1ΔC^{K99R} (lane e: 5 nM) and Fml1ΔC^{D196N} (lane f: 5 nM). The schematics represent X-12 and its dissociation products with the asterisk indicating the position of the 5′-end ^{32}P-label. See 'Materials and Methods' section for further details.

producing a single complex at low protein concentrations and two additional more retarded complexes at higher concentrations (Figure 2A). As shown previously, wild-type Fml1ΔC readily dissociates X-12 into flayed duplexes in the presence of Mg^{2+} and ATP (Figure 2B, lanes b–d). In contrast, both mutant proteins are unable to dissociate X-12 (Figure 2B, lanes e and f). These data show that K99R and D196N mutations have no affect on Fml1ΔC's ability to bind junction DNA but do abolish its ability to unwind them.

Fml1ΔC^{K99R} and Fml1ΔC^{D196N} are defective for fork regression

In addition to unwinding junctions, Fml1ΔC can also catalyse the regression of model replication forks (15). This process involves branch point migration through homologous DNA and could potentially be promoted by protein–DNA interactions in the absence of ATP hydrolysis. Indeed, previous studies of ATPase-deficient mutants of human FANCM have suggested that this

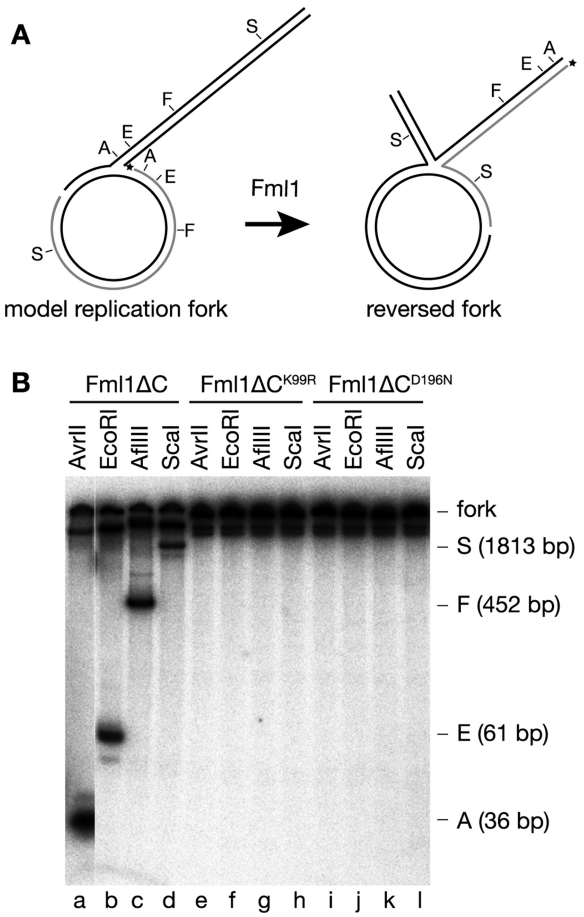

Figure 3. The catalysis of fork regression by wild-type and mutant Fml1ΔCs. (**A**) Schematic showing the model replication fork and its regression catalysed by Fml1. Letters A, E, F and S are the cleavage sites for *Avr*II, *Eco*RI, *Afl*III and *Sca*I, respectively. The asterisk indicates the position of the 5′-end ^{32}P-label on what is the equivalent of the nascent lagging strand. (**B**) Comparison of fork regression catalysed by Fml1ΔC (lanes a–d), Fml1ΔC^{K99R} (lanes e–h) and Fml1ΔC^{D196N} (lanes i–l). See 'Materials and Methods' section for further details.

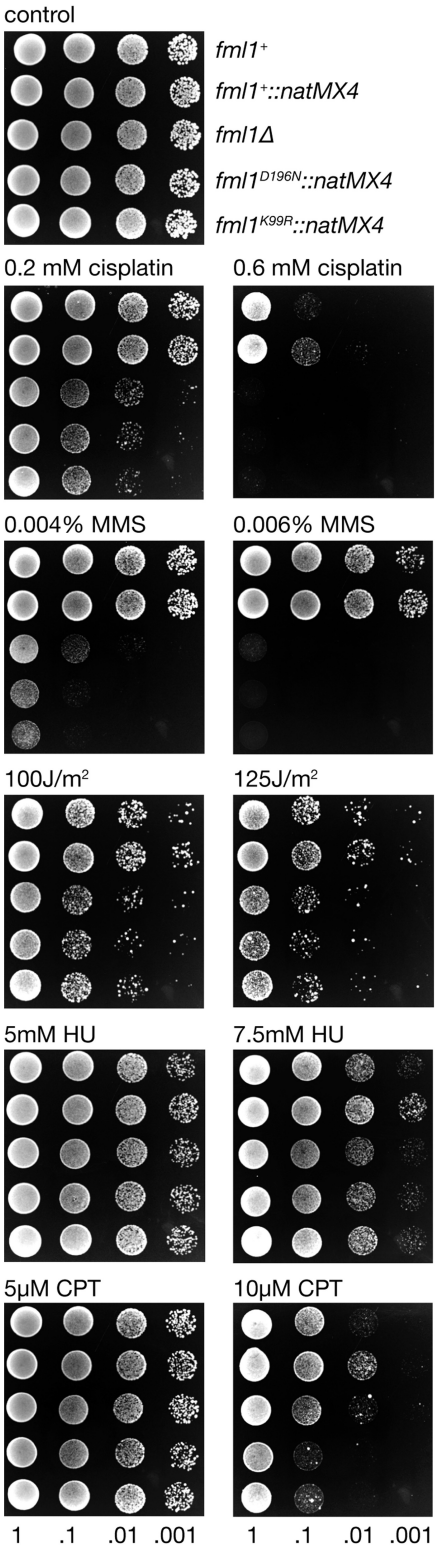

Figure 4. Spot assays comparing the genotoxin sensitivities of strains MCW1221, MCW4581, MCW2080, MCW4778 and MCW4779.

activity might not be wholly dependent on an ability to hydrolyse ATP (17). It was therefore important that Fml1ΔC^{K99R} and Fml1ΔC^{D196N} were tested to see whether they similarly retained an ability to catalyse this reaction. For this we used a model replication fork, which when regressed contains an extruded duplex DNA arm with 5′-end radiolabel (Figure 3A). The extent of fork reversal can be monitored by the ability to cleave the extruded arm with different restriction enzymes. As expected wild-type Fml1ΔC readily catalyses fork reversal with branch point migration occurring over distances of up to 1813 bp or more (Figure 3B, lanes a–d). In contrast, both Fml1ΔC^{K99R} and Fml1ΔC^{D196N} exhibit no detectable fork reversal activity even over relatively short distances of 36 bp (Figure 3B; lanes e–h and i–l). This deficiency in catalysing fork regression is not caused by an inability to bind fork DNA because both mutant proteins display similar binding as wild-type Fml1ΔC to a model replication fork (Supplementary Figure S3). Together these data indicate that the catalysis of fork reversal by Fml1ΔC *in vitro* depends on its ability to hydrolyse ATP.

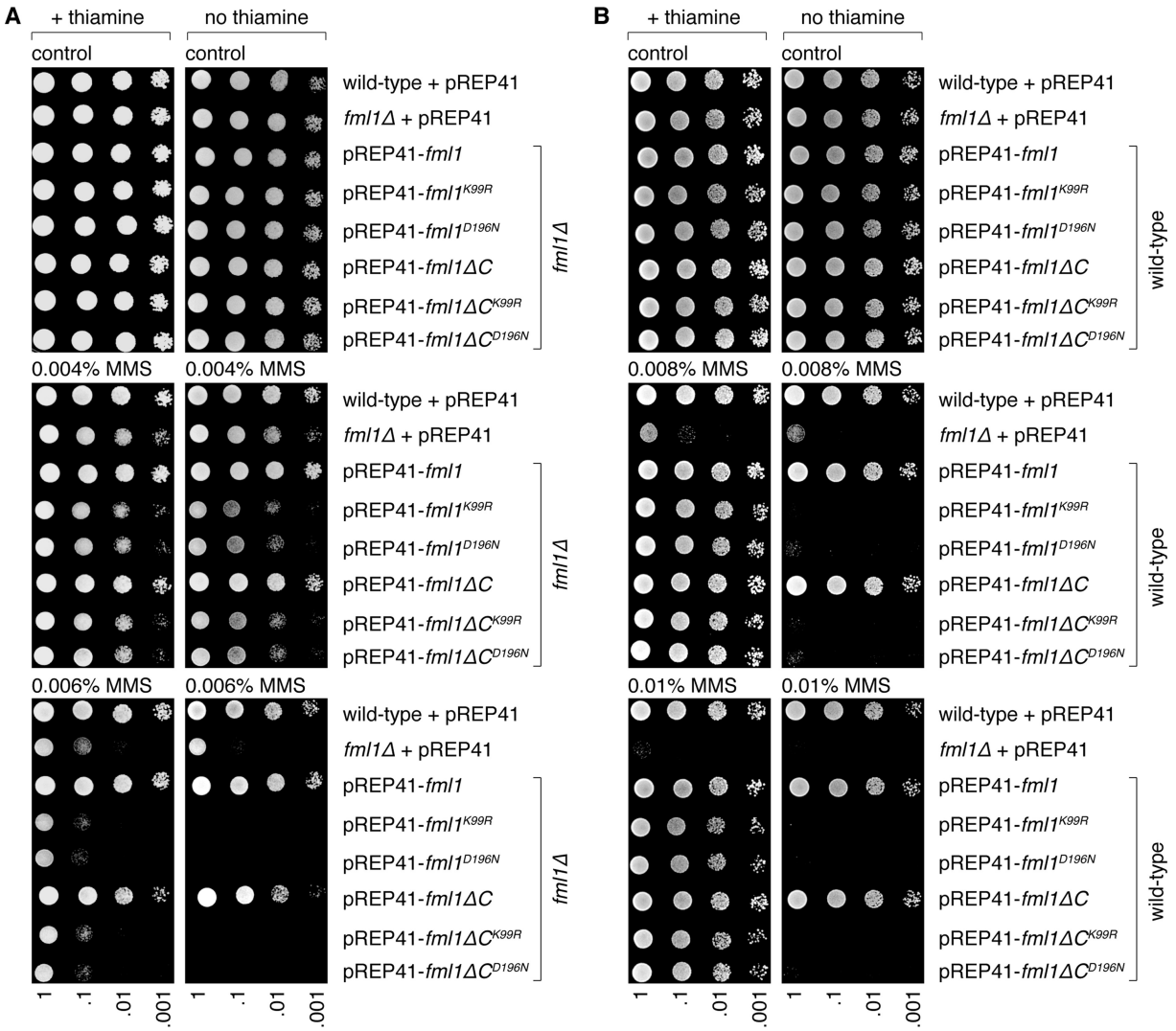

Figure 5. Spot assays comparing the MMS sensitivities of wild-type (MCW1221) and *fml1*Δ (MSW2080) strains carrying the indicated plasmids. Spot assays in A were photographed after 4 days growth at 30°C, whereas those in B were photographed after 5 days.

Genotoxin sensitivity of *fml1*^{K99R} and *fml1*^{D196N} mutants

Having established that Fml1ΔC^{K99R} and Fml1ΔC^{D196N} are deficient in ATP hydrolysis, junction unwinding and junction branch migration *in vitro,* we next investigated their function *in vivo*. To do this, the endogenous *fml1* gene was replaced with the mutant versions linked to a downstream *natMX4* marker (*fml1*^{K99R}::*natMX4* and *fml1*^{D196N}::*natMX4*). To control for any effects of the marker, a strain containing *fml1*$^{+}$ with *natMX4* downstream was also constructed (*fml1*$^{+}$::*natMX4*).

We have previously shown that a strain in which *fml1*$^{+}$ is deleted (*fml1*Δ) exhibits hypersensitivity to cisplatin and MMS (15). To assess the impact of the K99R and D196N mutations on genotoxin sensitivity, we performed a spot assay in which serial dilutions of the relevant strains were spotted onto complete media with or without genotoxin (Figure 4). Consistent with our previous data, the *fml1*Δ mutant exhibits hypersensitivity to cisplatin and MMS but is as resistant as wild-type to hydroxyurea (HU) and the topoisomerase I poison camptothecin (CPT). We also observed a slight hypersensitivity to high doses of ultraviolet light (UV), which had been missed in our previous study. Both point mutants are similarly sensitive to cisplatin and UV as the deletion strain and slightly more sensitive to MMS (Figure 4). Intriguingly, and unlike the deletion mutant, they are also modestly hypersensitive to CPT. These sensitivities can be directly attributed to the point mutations in *fml1* rather than the linked *natMX4* marker because the *fml1*$^{+}$::*natMX4* strain exhibits no hypersensitivity to any of the genotoxins used here (Figure 4). In fact it is slightly more resistant than the wild-type strain from which it was derived. The reason for this enhanced resistance is currently unclear. Overall these data show that Fml1's ATPase activity is essential for its ability to promote DNA damage repair/tolerance. The heightened sensitivity of the ATPase-deficient mutants suggests that they retain the ability to bind their intended substrates *in vivo* and in so-doing block other alternative repair/tolerance pathways.

Over-expression of Fml1^{K99R} and Fml1^{D196N} sensitizes both wild-type and *fml1*Δ strains to MMS

To further investigate the toxicity of Fml1^{K99R} and Fml1^{D196N}, we analysed the effect of their over-expression on MMS sensitivity in wild-type and *fml1*Δ mutant strains. The thiamine repressible *nmt41* promoter in plasmid pREP41 was used to drive over-expression (24), and MMS sensitivity was assessed by spot assays (Figure 5). Consistent with previous data, plasmid-borne *fml1*$^{+}$ and *fml1*Δ*C* efficiently complement the MMS sensitivity of a *fml1*Δ mutant when expressed from the *nmt41* promoter (Figure 5A) (note that the *nmt41* promoter is leaky and therefore still drives some expression even in the presence of thiamine) (15). As expected, expression of either full-length or C-terminally truncated Fml1 K99R and D196N mutants failed to rescue MMS sensitivity, confirming that ATP hydrolysis is essential for Fml1's role in promoting genotoxin resistance. Moreover, in the absence of thiamine (i.e. when the *nmt41* promoter is de-repressed), they actually increased *fml1*Δ mutant sensitivity (Figure 5A). Over-expression of either full-length or C-terminally truncated Fml1^{K99R}/Fml1^{D196N} also sensitized wild-type cells to MMS and importantly the degree of sensitization was slightly greater than seen in a *fml1*Δ strain carrying the empty pREP41 plasmid (Figure 5B, compare the sensitivity of strains to 0.008% MMS in the absence of thiamine). Altogether these data suggest that over-expression of ATPase-deficient Fml1 (with or without its C-terminal domain) can interfere both with endogenous wild-type Fml1 and other repair/tolerance pathways in their response to MMS-induced damage.

Fml1^{K99R}-GFP and Fml1^{D196N}-GFP form detectable nuclear foci following MMS treatment

To investigate whether Fml1^{K99R}/Fml1^{D196N} persists at sites on DNA following MMS-induced damage, we constructed strains that express wild-type/mutant Fml1 with a C-terminal green fluorescent protein (GFP) fusion from the endogenous *fml1* promoter. All three strains express similar levels of the fusion protein and exhibit the same MMS sensitivity as the equivalent strain without GFP (data not shown). Cells were exposed to MMS for 4 h and then monitored for the appearance of nuclear foci during a 6-h recovery period. In cells expressing the Fml1^{+}-GFP fusion, only background fluorescence was detected both in the absence of MMS and following MMS exposure (Figure 6B and data not shown). The same was true for cells expressing Fml1$^{K99R/D196N}$-GFP in the absence of MMS; however, weak nuclear foci were detected in up to 14% of cells at the 3–6 h time points during the recovery period following MMS exposure (Figure 6A and B). In almost all these cases, only a single focus was detected in each nucleus. These data show that, in contrast to wild-type Fml1, Fml1$^{K99R/D196N}$ can accumulate at sites on DNA and persist there long enough for foci to be detected.

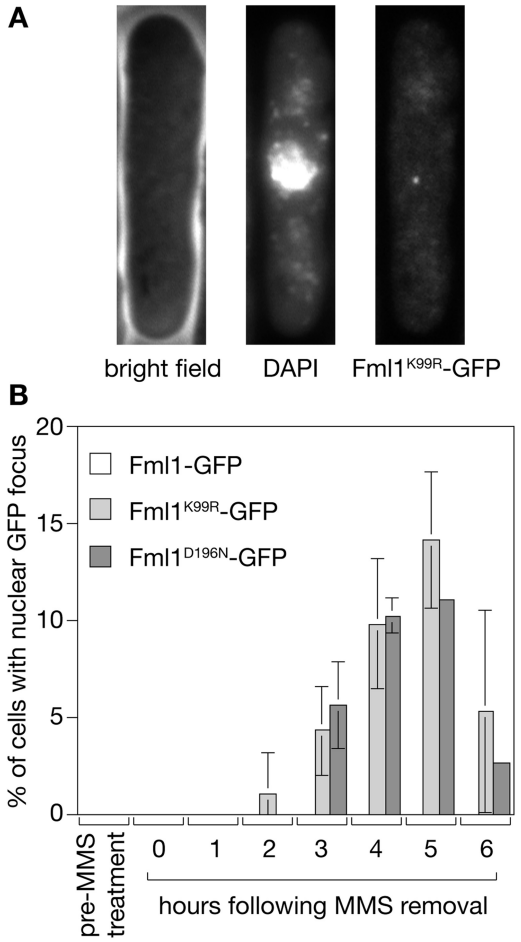

Figure 6. Induction of Fml1^{K99R}-GFP and Fml1^{D196N}-GFP foci by MMS. (**A**) Example of a cell with a Fml1^{D196N}-GFP focus. DNA was stained with DAPI. (**B**) Percentage of cells with a nuclear GFP focus. Values are the mean of two to three independent experiments except for the Fml1^{D196N}-GFP 5- and 6-h time points, which are from a single experiment. In each experiment >100 cells were analysed for each time point. Error bars represent the range.

fml1^{K99R} and *fml1*^{D196N} mutants exhibit elevated levels of crossing over resulting from mitotic DSB repair

We have shown previously that a *fml1*Δ strain exhibits high levels of crossing over in a plasmid gap repair assay (15). This assay involves transformation of a plasmid, which has been cut to generate a 153 bp double-stranded gap within a copy of *ade6*, into a strain containing a mutant allele of *ade6* (*ade6-M26*) at its normal genomic locus on chromosome III. The linearized plasmid is repaired *in vivo* by HR, with the chromosomal *ade6-M26* acting as the donor of genetic information during the reaction (Figure 7A). In wild-type cells, the majority of the repaired plasmids (~75%) contain a fully restored *ade6*$^{+}$ gene through gene conversion with chromosomal *ade6-M26*, and most of these (~90%) are non-crossovers, where the plasmid has re-circularized (Figure 7A, C and D). A *fml1*Δ mutant exhibits similar levels of plasmid repair and Ade^{+} recombinants as wild-type (Figure 7B and C), but unlike wild-type >30% of the recombinants are crossovers, where the plasmid has

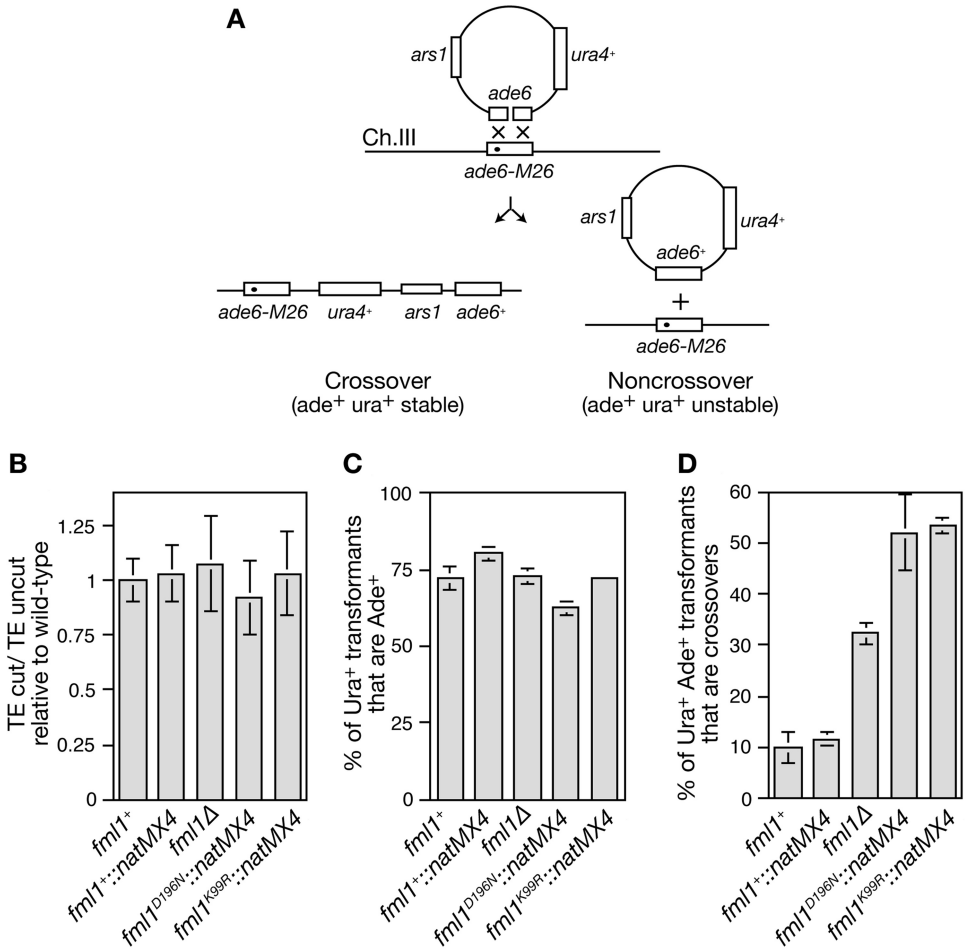

Figure 7. Comparison of wild-type and *fml1* mutant strains in the plasmid gap repair assay. (**A**) Schematic showing the repair of a double-strand gap in *ade6* on a plasmid by HR with *ade6-M26* on chromosome III. The *M26* mutation is indicated by the filled circle. (**B**) Histogram showing the mean relative transformation efficiency (TE) of cut versus uncut plasmid in strains MCW1193, MCW4893, MCW2096, MCW4894 and MCW4895. (**C**) Histogram showing the percentage of Ura^+ transformants that are Ade^+ recombinants in the same strains as in (B). (**D**) Histogram showing the percentage of Ade^+ recombinants that are crossovers in the same strains as in (B). Error bars are the standard deviations about the mean.

integrated into the chromosome (Figure 7D). Intriguingly when *fml1*^{K99R} and *fml1*^{D196N} mutants were tested in the same assay an even greater proportion (~50%) of Ade^+ recombinants were found to be crossovers (Figure 7D). This difference is not due to the linked *natMX4* marker as a *fml1*$^+$::*natMX4* strain behaves like the parental wild-type strain in this assay (Figure 7B–D). Altogether these data show that an ability to hydrolyse ATP is critical for Fml1's role in promoting crossover avoidance during mitotic DSB repair. Moreover, similar to our finding with the genotoxin sensitivity assay, both point mutants appear to retain some function *in vivo*, which in this case impedes alternative non-crossover pathways yet is seemingly permissive for the crossover pathway(s).

fml1^{K99R} and *fml1*^{D196N} are deficient for promoting gene conversion at stalled replication forks

Fml1 promotes Rad51-dependent gene conversion between a direct repeat of *ade6*$^-$ mutant heteroalleles especially when a *RTS1* polar replication fork barrier (RFB) is positioned between the repeats to stall fork progression (15). On the basis of this observation and Fml1's capabilities *in vitro,* we have proposed that Fml1 promotes recombination at stalled replication forks by catalysing their reversal, which generates a substrate for recombinases to act on (15). If true then both $Fml1^{K99R}$ and $Fml1^{D196N}$, which are totally deficient in catalysing fork reversal *in vitro*, should be unable to promote recombination *in vivo*. To test this we compared the *fml1*^{K99R} and *fml1*^{D196N} strains to wild-type control and *fml1*Δ strains using the *RTS1*-induced direct repeat recombination assay shown in Figure 8A. In this assay, recombination between the two *ade6*$^-$ genes is induced by replication fork stalling at *RTS1* and gives rise to two classes of Ade^+ recombinant–conversion-types, which retain an intervening *his3*$^+$ gene, and deletion-types, which lose it. In the *fml1*$^+$ strain, the frequency of conversion- and deletion-types are both in the range of $120–150 \times 10^{-4}$, and in the *fml1*$^+$::*natMX4* strain, they are slightly higher at $\sim 200 \times 10^{-4}$ (Figure 8B and C). Both *fml1* null and point mutants yield a similar level of deletion types as the *fml1*$^+$ strain (Figure 8C). However, all three mutants show a similar ~10-fold decrease in the frequency of conversion-types compared to the

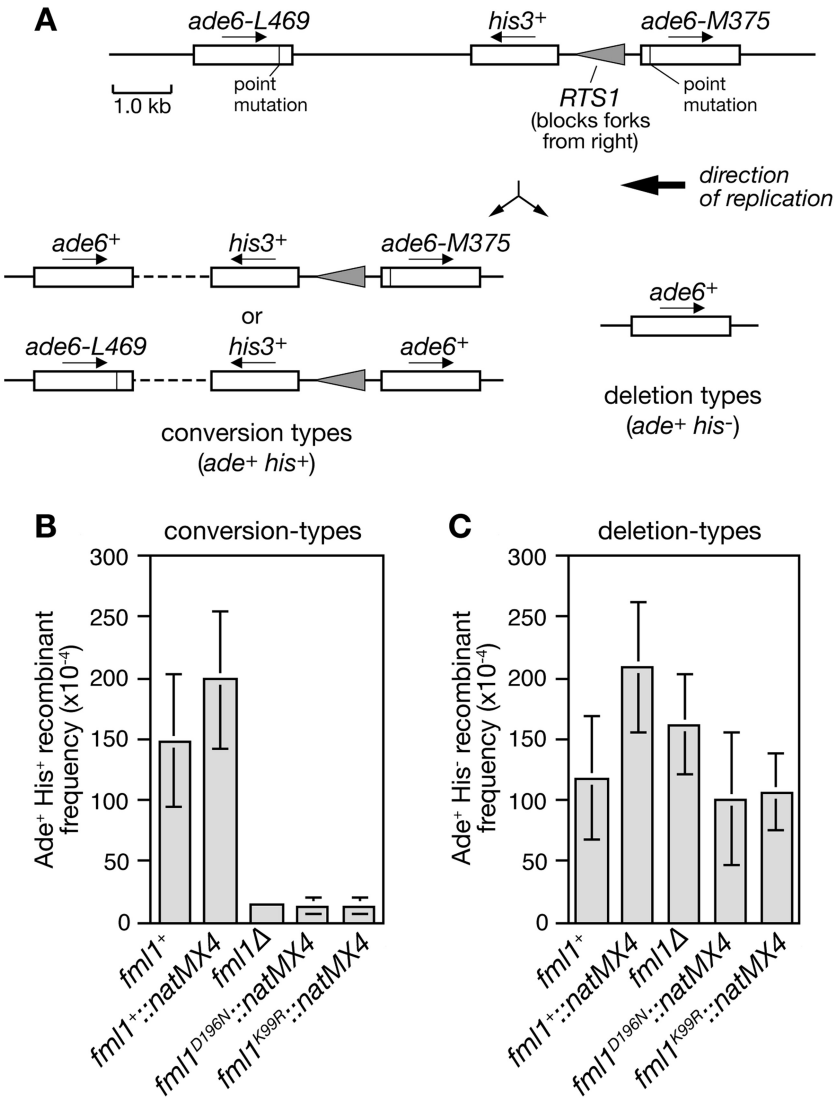

Figure 8. *RTS1*-induced direct repeat recombination in wild-type and *fml1* mutant strains. (**A**) Schematic showing the direct repeat recombination substrate on chromosome III plus the two classes of Ade^+ recombinant product. (**B**) Ade^+ His^+ (conversion-types) recombinant frequencies for strains MCW4713, MCW4797, MCW3061, MCW4801 and MCW4780. (**C**) Ade^+ His^- (deletion-types) recombinant frequencies for the same strains as in (B). In both (B) and (C), the error bars represent the standard deviations about the mean.

fml1$^+$ strain (Figure 8B). These data show that Fml1's ATPase activity, which is integral to its ability to catalyse replication fork reversal, is essential for promoting Rad51-dependent recombination at stalled replication forks.

DISCUSSION

We have shown that Fml1's ability to hydrolyse ATP is essential for its function in promoting repair/tolerance of DNA damage, crossover avoidance during DSB repair and Rad51-dependent gene conversion at a blocked replication fork. As Fml1 uses ATP hydrolysis to fuel its unwinding and branch migration of junction DNA it is likely that these activities are central to its aforementioned roles. Importantly mutants that are defective in ATP hydrolysis display wild-type levels of junction DNA binding *in vitro*, and therefore simply binding to its proposed substrates *in vivo* is not sufficient for Fml1 to perform its DNA repair and recombinogenic functions.

Similar to our findings, studies of FANCM in human cells have shown that a K117R mutation in helicase motif 1, which is equivalent to K99R in Fml1, results in a deficiency in cisplatin resistance (7,21). Interestingly this mutation does not impair FANCM's ability to promote the monoubiquitination and localization into DNA repair foci of FANCD2 (7,21). These data indicate that FANCM can serve at least two functions in promoting DNA repair: (i) it binds DNA and thereby can act as a scaffold for the recruitment of the FA core complex to chromatin; and (ii) it can use the energy from hydrolysing ATP to branch migrate and unwind junction DNA, which can potentially promote ICL repair in various ways as discussed earlier. Our observation that ATPase-dead Fml1

mutants exhibit no residual DNA repair capacity suggests that in *S. pombe* Fml1 does not play an important scaffolding role, which is in line with the apparent absence of other FA pathway proteins.

The idea that ATP hydrolysis is needed for FANCM to promote ICL repair has been questioned following the observation that a D203A mutation in helicase motif II failed to cause hypersensitivity to cisplatin in chicken DT40 cells (12). Like the K117R mutation in motif I, the D203A mutation destroys ATPase activity; however, unlike K117R it is thought not to impair ATP binding. Based on this it was proposed that FANCM's motor activity is unnecessary for promoting DNA crosslink repair, which instead simply relies on a conformational change in FANCM brought about by binding ATP (12). However, our data show that a D196N mutation in Fml1, which is the equivalent residue as D203 in chicken FANCM, produces a null mutant phenotype with respect to cisplatin sensitivity. This suggests that ATP binding on its own is not sufficient in the case of the fission yeast FANCM orthologue for it to perform its role in DNA repair.

One intriguing observation that we have made is that both *fml1*^{K99R} and *fml1*^{D196N} mutants in some cases exhibit phenotypes that are more extreme than those of the null mutant. Namely they are more sensitive to MMS, exhibit hypersensitivity to CPT that is not seen with the null mutant and display higher levels of crossing over in the plasmid gap repair assay. Over-expression of these Fml1 mutants also sensitizes wild-type cells to MMS to a greater degree than deleting *fml1* and increases the hypersensitivity of a *fml1*Δ mutant. These data suggest that Fml1^{K99R} and Fml1^{D196N} retain a function *in vivo* that blocks alternative DNA processing pathways. For example, MMS is known to cause lesions that block replication fork progression (35), and Fml1's normal role here may be to promote lesion bypass through catalysing fork reversal (15). Presumably, the mutant proteins would bind to stalled forks, as they do *in vitro*, and in so doing impede other mechanisms of repair or lesion tolerance, such as TLS or those that rely on alternative fork reversal pathways. In this respect, it is worth noting that a *fml1*Δ mutant, similar to a *mph1*Δ mutant in *S. cerevisiae*, exhibits a hyper-mutator phenotype indicating increased usage of TLS to tolerate replication fork blocking lesions (36). Furthermore, loss of Fml1 also results in greater reliance on Rad8 for survival in the presence of MMS (15). Rad8 is the orthologue of *S. cerevisiae* Rad5, which is a key component of the error-free branch of the post-replication repair pathway and has been proposed to catalyse fork reversal (32). Evidence that Fml1^{K99R}/Fml1^{D196N} might persist on DNA following MMS-induced damaged comes from our observation that both mutant proteins when fused to GFP form detectable nuclear foci following exposure to MMS, whereas wild-type Fml1 does not. However, these foci are only detected 3 h after MMS is removed, which is not consistent with Fml1^{K99R}/Fml1^{D196N} accumulating at replication forks when they first stall during S-phase. Possibly Fml1 is recruited later to a subset of 'problem' replication forks that persist into the G2 and M phases of the cell cycle.

Binding to its substrate and preventing its normal processing may also account for the increased levels of crossing over during DSB repair in *fml1*^{K99R} and *fml1*^{D196N} mutants. In this case, the substrate is most likely a D-loop that is formed by Rad51-mediated strand invasion. By binding to the D-loop Fml1^{K99R}/Fml1^{D196N} could prevent its maturation into a double HJ, which is a substrate for the dissolution pathway that appears to be the main alternative to SDSA for avoiding crossovers (15,37). In the absence of both major non-crossover pathways, D-loops could be resolved by junction-specific endonucleases such as Mus81-Eme1 that generate crossover recombinants (15,38). Indeed, a *mus81*Δ *fml1*Δ double mutant exhibits a synthetic reduction in viability and enhanced genotoxin sensitivity consistent with the idea that Mus81 and Fml1 function in alternative pathways for processing D-loops (15). Seemingly, the presence of Fml1^{K99R}/Fml1^{D196N} at the D-loop is not a barrier to Mus81-Eme1 and might even aid it by holding it in a confirmation that is amenable to cleavage. Future *in vitro* studies may provide insight into how these enzymes compete for the same substrate.

SUPPLEMENTARY DATA

Supplementary Data are available at NAR Online: Supplementary Figures 1–3.

ACKNOWLEDGEMENTS

The authors thank Leonard Wu (University of Oxford) for providing the plasmids for constructing the model replication fork and their lab members Fekret Osman and Sonali Bhattacharjee for providing strains, Vincent Mason for technical assistance and Fekret Osman, Alexander Lorenz and Roland Steinacher for critical reading of the manuscript.

FUNDING

The Wellcome Trust [090767/Z/09/Z]; K. Pathak Clarendon Scholarship from Exeter College, University of Oxford (to S.N.). Funding for open access charge: The Wellcome Trust.

Conflict of interest statement. None declared.

REFERENCES

1. Whitby,M.C. (2010) The FANCM family of DNA helicases/translocases. *DNA Repair*, **9**, 224–236.
2. Meetei,A.R., Medhurst,A.L., Ling,C., Xue,Y., Singh,T.R., Bier,P., Steltenpool,J., Stone,S., Dokal,I., Mathew,C.G. *et al.* (2005) A human ortholog of archaeal DNA repair protein Hef is defective in Fanconi anemia complementation group M. *Nat. Genet.*, **37**, 958–963.
3. Levitus,M., Joenje,H. and de Winter,J.P. (2006) The Fanconi anemia pathway of genomic maintenance. *Cell. Oncol.*, **28**, 3–29.

4. Moldovan,G.L. and D'Andrea,A.D. (2009) How the Fanconi Anemia Pathway Guards the Genome. *Annu. Rev. Genet.*, **43**, 223–249.
5. Wang,W. (2007) Emergence of a DNA-damage response network consisting of Fanconi anaemia and BRCA proteins. *Nat. Rev. Genet.*, **8**, 735–748.
6. Kim,J.M., Kee,Y., Gurtan,A. and D'Andrea,A.D. (2008) Cell cycle-dependent chromatin loading of the Fanconi anemia core complex by FANCM/FAAP24. *Blood*, **111**, 5215–5222.
7. Xue,Y., Li,Y., Guo,R., Ling,C. and Wang,W. (2008) FANCM of the Fanconi anemia core complex is required for both monoubiquitination and DNA repair. *Hum. Mol. Genet.*, **17**, 1641–1652.
8. Collis,S.J., Ciccia,A., Deans,A.J., Horejsi,Z., Martin,J.S., Maslen,S.L., Skehel,J.M., Elledge,S.J., West,S.C. and Boulton,S.J. (2008) FANCM and FAAP24 function in ATR-mediated checkpoint signaling independently of the Fanconi anemia core complex. *Mol. Cell*, **32**, 313–324.
9. Huang,M., Kim,J.M., Shiotani,B., Yang,K., Zou,L. and D'Andrea,A.D. (2010) The FANCM/FAAP24 complex is required for the DNA interstrand crosslink-induced checkpoint response. *Mol. Cell*, **39**, 259–268.
10. Schwab,R.A., Blackford,A.N. and Niedzwiedz,W. (2010) ATR activation and replication fork restart are defective in FANCM-deficient cells. *EMBO J.*, **29**, 806–818.
11. Bakker,S.T., van de Vrugt,H.J., Rooimans,M.A., Oostra,A.B., Steltenpool,J., Delzenne-Goette,E., van der Wal,A., van der Valk,M., Joenje,H., te Riele,H. *et al.* (2009) FancM-deficient mice reveal unique features of Fanconi anemia complementation group M. *Hum. Mol. Genet.*, **18**, 3484–3495.
12. Rosado,I.V., Niedzwiedz,W., Alpi,A.F. and Patel,K.J. (2009) The Walker B motif in avian FANCM is required to limit sister chromatid exchanges but is dispensable for DNA crosslink repair. *Nucleic Acids Res.*, **37**, 4360–4370.
13. Deans,A.J. and West,S.C. (2009) FANCM connects the genome instability disorders Bloom's Syndrome and Fanconi Anemia. *Mol. Cell*, **36**, 943–953.
14. Prakash,R., Satory,D., Dray,E., Papusha,A., Scheller,J., Kramer,W., Krejci,L., Klein,H., Haber,J.E., Sung,P. *et al.* (2009) Yeast Mph1 helicase dissociates Rad51-made D-loops: implications for crossover control in mitotic recombination. *Genes Dev.*, **23**, 67–79.
15. Sun,W., Nandi,S., Osman,F., Ahn,J.S., Jakovleska,J., Lorenz,A. and Whitby,M.C. (2008) The fission yeast FANCM ortholog Fml1 promotes recombination at stalled replication forks and limits crossing over during double-strand break repair. *Mol. Cell*, **32**, 118–128.
16. Gari,K., Decaillet,C., Delannoy,M., Wu,L. and Constantinou,A. (2008) Remodeling of DNA replication structures by the branch point translocase FANCM. *Proc. Natl Acad. Sci. USA*, **105**, 16107–16112.
17. Gari,K., Decaillet,C., Stasiak,A.Z., Stasiak,A. and Constantinou,A. (2008) The Fanconi anemia protein FANCM can promote branch migration of Holliday junctions and replication forks. *Mol. Cell*, **29**, 141–148.
18. Zheng,X.F., Prakash,R., Saro,D., Longerich,S., Niu,H. and Sung,P. (2011) Processing of DNA structures via DNA unwinding and branch migration by the *S. cerevisiae* Mph1 protein. *DNA Repair*, **10**, 1034–1043.
19. Svendsen,J.M. and Harper,J.W. (2010) GEN1/Yen1 and the SLX4 complex: Solutions to the problem of Holliday junction resolution. *Genes Dev.*, **24**, 521–536.
20. Yan,Z., Delannoy,M., Ling,C., Daee,D., Osman,F., Muniandy,P.A., Shen,X., Oostra,A.B., Du,H., Steltenpool,J. *et al.* (2010) A histone-fold complex and FANCM form a conserved DNA-remodeling complex to maintain genome stability. *Mol. Cell*, **37**, 865–878.
21. Singh,T.R., Bakker,S.T., Agarwal,S., Jansen,M., Grassman,E., Godthelp,B.C., Ali,A.M., Du,C.H., Rooimans,M.A., Fan,Q. *et al.* (2009) Impaired FANCD2 monoubiquitination and hypersensitivity to camptothecin uniquely characterize Fanconi anemia complementation group M. *Blood*, **114**, 174–180.
22. Goldstein,A.L. and McCusker,J.H. (1999) Three new dominant drug resistance cassettes for gene disruption in *Saccharomyces cerevisiae*. *Yeast*, **15**, 1541–1553.
23. Bahler,J., Wu,J.Q., Longtine,M.S., Shah,N.G., McKenzie,A. 3rd, Steever,A.B., Wach,A., Philippsen,P. and Pringle,J.R. (1998) Heterologous modules for efficient and versatile PCR-based gene targeting in *Schizosaccharomyces pombe*. *Yeast*, **14**, 943–951.
24. Maundrell,K. (1993) Thiamine-repressible expression vectors pREP and pRIP for fission yeast. *Gene*, **123**, 127–130.
25. Moreno,S., Klar,A. and Nurse,P. (1991) Molecular genetic analysis of fission yeast *Schizosaccharomyces pombe*. *Methods Enzymol.*, **194**, 795–823.
26. Ahn,J.S., Osman,F. and Whitby,M.C. (2005) Replication fork blockage by *RTS1* at an ectopic site promotes recombination in fission yeast. *EMBO J.*, **24**, 2011–2023.
27. Osman,F. and Whitby,M.C. (2009) Monitoring homologous recombination following replication fork perturbation in the fission yeast *Schizosaccharomyces pombe*. *Methods Mol. Biol.*, **521**, 535–552.
28. Baykov,A.A., Evtushenko,O.A. and Avaeva,S.M. (1988) A malachite green procedure for orthophosphate determination and its use in alkaline phosphatase-based enzyme immunoassay. *Anal. Biochem.*, **171**, 266–270.
29. Whitby,M.C. and Dixon,J. (1997) A new Holliday junction resolving enzyme from *Schizosaccharomyces pombe* that is homologous to CCE1 from *Saccharomyces cerevisiae*. *J. Mol. Biol.*, **272**, 509–522.
30. Whitby,M.C. and Dixon,J. (1998) Substrate specificity of the SpCCE1 holliday junction resolvase of *Schizosaccharomyces pombe*. *J. Biol. Chem.*, **273**, 35063–35073.
31. Whitby,M.C., Osman,F. and Dixon,J. (2003) Cleavage of model replication forks by fission yeast Mus81-Eme1 and budding yeast Mus81-Mms4. *J. Biol. Chem.*, **278**, 6928–6935.
32. Blastyak,A., Pinter,L., Unk,I., Prakash,L., Prakash,S. and Haracska,L. (2007) Yeast Rad5 protein required for postreplication repair has a DNA helicase activity specific for replication fork regression. *Mol. Cell*, **28**, 167–175.
33. Ralf,C., Hickson,I.D. and Wu,L. (2006) The Bloom's syndrome helicase can promote the regression of a model replication fork. *J. Biol. Chem.*, **281**, 22839–22846.
34. West,S.C. (1995) Holliday junctions cleaved by Rad1? *Nature*, **373**, 27–28.
35. Larson,K., Sahm,J., Shenkar,R. and Strauss,B. (1985) Methylation-induced blocks to *in vitro* DNA replication. *Mutat. Res.*, **150**, 77–84.
36. Schurer,K.A., Rudolph,C., Ulrich,H.D. and Kramer,W. (2004) Yeast MPH1 gene functions in an error-free DNA damage bypass pathway that requires genes from Homologous recombination, but not from postreplicative repair. *Genetics*, **166**, 1673–1686.
37. Wu,L. and Hickson,I.D. (2003) The Bloom's syndrome helicase suppresses crossing over during homologous recombination. *Nature*, **426**, 870–874.
38. Osman,F., Dixon,J., Doe,C.L. and Whitby,M.C. (2003) Generating crossovers by resolution of nicked Holliday junctions: a role for Mus81-Eme1 in meiosis. *Mol. Cell*, **12**, 761–774.